



Determination of heterogeneous electron transfer rate constants at interdigitated nanoband electrodes fabricated by an optical mix-and-match process



Francisco Javier del Campo^{a,*}, Llibertat Abad^a, Xavi Illa^{a,b}, Elisabet Prats-Alfonso^{a,b}, Xavier Borrís^c, Josep Maria Cirera^a, Huei-Yu Bai^d, Yu-Chen Tsai^d

^a Instituto de Microelectrónica de Barcelona, IMB-CNM (CSIC), Esfera UAB, Campus Universitat Autònoma de Barcelona, 08193 Bellaterra, Barcelona, Spain

^b CIBER-BBN, Networking Center on Bioengineering, Biomaterials and Nanomedicine, Zaragoza, Spain

^c Institut Català de Nanociència i Nanotecnologia (ICN2), UAB Campus, ICN2 Building, 08193 Bellaterra, Barcelona, Spain

^d Department of Chemical Engineering, National Chung Hsing University, 250, Kuo Kuang Road, Taichung 402, Taiwan

ARTICLE INFO

Article history:

Received 3 November 2013

Accepted 4 December 2013

Available online 26 December 2013

Keywords:

Microband electrodes

Redox cycling

Generator–collector experiments

Electrochemical simulation

Electrode kinetics

Microfabrication

ABSTRACT

Interdigitated microband electrodes are important electroanalytical tools, and have been used in the construction of advanced sensing and biosensing devices for a long time. Nanoband-based systems, on the other hand, are more difficult to come by, as their fabrication involves the use of costly and scarce e-beam lithography resources. In this work we present the fabrication of interdigitated nanobands down to 400 nm using optical techniques exclusively. The process combines a step-and-repeat process to define Cr–Au nano- and microbands, and a standard lithography to pattern the active areas and contacts through an SU-8 passivation layer. This work presents the physical and electrochemical characterization of these devices, and our results also show that generator–collector experiments at these nanometric devices can be used in conventional electroanalytical applications, but also to measure electrode kinetics. While electrode kinetics does not affect collection efficiency to a great extent, the fast mass transport rates achieved at these devices makes the voltammetric current critically dependent on electron transfer rates.

© 2013 Elsevier B.V. All rights reserved.

1. Introduction

Narrow microband electrodes are valuable electroanalytical tools because nonlinear diffusion to their edges allows them to display fast mass transport rates and quasi-steady state currents; microband electrodes also display low capacitive currents, and their small areas result in smaller *iR* drop effects. These factors combined result in high sensitivities and signal-to-noise ratios, [1] and are the reason why single microband electrodes are commonly used as detectors in channel cells [2–5] and lab-on-a-chip systems [6–10].

However, the possibility to work with two or more closely spaced microbands that can be polarized independently has made interdigitated microband electrodes one of the most frequent micro- and nano-electrode geometries used in electroanalytical applications [11–14]. They have been applied to the study of fast chemical reactions coupled to redox processes [15–18], to the determination of diffusion coefficients [19], to the development of

highly sensitive electrochemical biosensors [20,21], and even to the selective detection of electroactive species with close formal potentials [22]. Although interdigitated microband arrays are very vulnerable to *iR*-drop effects at high current levels (in the μA range), they have nevertheless been used as detectors in flow systems such as liquid chromatographs [23] and, more recently, integrated in lab-on-a-chip devices.

Interdigitated structures can be fabricated by different methods, including screen printing [24,25], lamination [26], photolithography [27–29], and maskless techniques such as e-beam [30], focused ion beam [31], and nanoimprint lithography [32–38]. Although mask-less techniques in principle enable the fabrication of nanometric structures, these techniques are generally plagued with problems including higher cost, lower throughput, and lower yields than optical lithographic techniques.

On the other hand, although smaller features may be accessible [15,29], microfabrication using standard UV–vis optical lithography commonly stops at critical dimensions around 1 μm and commercial interdigitated microband electrodes typically present pitch distances of 4 μm or bigger.

Regarding the electrochemical response of microband electrodes and their arrays, Aoki developed expressions that describe

* Corresponding author. Tel.: +34 93 594 77 00x2406; fax: +34 93 580 14 96.
E-mail address: javier.delcampo@csic.es (F.J. del Campo).

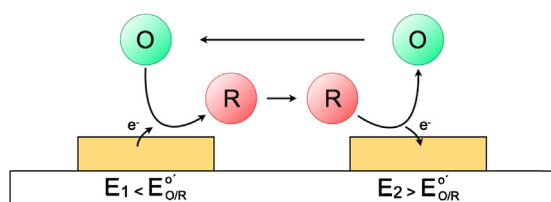


Fig. 1. Diagrammatic representation of the generator–collector experiment. An electroactive species, O , is reduced at one set of microbands. The product, R , then diffuses and is reduced back at the adjacent set, which is polarized at a potential above the formal potential of the O/R couple.

the short [39] and long time [39] chronoamperometric response and linear sweep voltammograms at single microband electrodes, as well as the steady-state diffusion-controlled current at interdigitated microband arrays operating in so-called generator–collector mode [40]. This mode of operation, schematized in Fig. 1, consists in the diffusional transport of an electroactive species generated at a “generator” microband towards an adjacent “collector” microband that is polarized so that the arriving species is transformed back to its original state. This species will then diffuse away from the “collector” towards the “generator” electrode, and the cycle repeats itself for as long as the electrodes are polarized. This is commonly known as “redox cycling”, and it offers important sensitivity and current enhancements [29,30,41–45]. Out of the parameters used to describe the “goodness” of interdigitated microband arrays, current efficiency is the most common. Other parameters that can be found are the number of redox cycles [45], and the shielding and feedback factors, S_F and F_F , respectively [15]. Collection efficiency, i_{eff} , is the ratio between the current registered at the collector and that registered at the generator ($i_{eff} = -i_{col}/i_{gen}$). The number of redox cycles, R_c , on the other hand, gives an idea of the number of times that species shuttle to and fro between adjacent microbands. It is defined as:

$$R_c = (1 - i_{eff}^2)^{-1}$$

The shielding and feedback factors also quantify the effect of neighbouring microbands when polarized at the same potential (shielding) or in generator–collector mode (feedback). As noted by Niwa, the accuracy of R_c (and by extension of S_F and F_F) is strongly dependent on the experimental error associated to the determination of i_{eff} [45]. Although collection efficiency depends largely on the distance between adjacent microbands, and smaller gaps result in greater efficiencies [15,45], the aspect ratio of the microbands also has an important effect on the observed collection efficiency, and closely spaced, protruding-microbands display the highest efficiencies [29,41].

The actual geometry of the microbands has a deep impact on the diffusion-controlled currents observed at interdigitated microelectrode arrays. The most important theoretical work reported to date on the behaviour of interdigitated microband electrodes considers planar systems [15,28,46,47]. However, as the gap between microbands narrows, especially in the case of nanoelectrodes, the microband “z” dimension becomes increasingly important. In the case of nanobands it is possible to find aspect ratios of 1 or more [29,41]. These devices can no longer be considered planar, and numerical simulations are required to understand their behaviour fully [41].

In this paper, we present the 4-in. silicon wafer level fabrication of interdigitated gold micro- and nanometric structures fabricated by optical lithographic techniques. These micro- and nano-bands were patterned by lift-off after a step-and-repeat lithographic process, while the active areas and contact pads on the passivation layer were defined in a mask aligner. These are regular interdigitated structures composed by 500 μm -long bands of

widths down to 400 nm, over an active area of 500 $\mu\text{m} \times 500 \mu\text{m}$. The gold microbands protrude 100 nm over the silicon surface which, given the width of the microbands, needs to be considered in simulations and data analysis. These new interdigitated microband electrodes display current collection efficiencies ranging between 93% and 98.7% depending on geometry, and redox cycle numbers between 19 (4 μm pitch) and 135 (800 nm pitch). These figures agree with theory, although the observed current levels were lower than expected due to quasi-reversible electron transfer kinetics. The electron transfer rate constant estimated for these electrodes was in line with that found at gold microelectrodes of other geometries fabricated by the same process. As we will show, generator collector experiments in combination with simulations can be used to successfully measure heterogeneous electron transfer rate constants.

2. Materials and methods

All solutions were prepared using deionised water of resistivity not less than 18 $\text{M}\Omega \text{ cm}$, and all chemicals used in this work were of analytical grade and were used as received without further purification. Potassium nitrate ($\geq 99.0\%$), Potassium hexacyanoferrate II (ReagentPlus, ≥ 98.5), acetone, 2-propanol, and ethanol (all 99.9%) were purchased from Sigma Aldrich, Spain. 3 M KCl (electrolyte solution for Ag/AgCl electrode, Metrohm, Spain), and Siotech MT 06/01 VLSI Selectipur (BASF, Spain).

Lithography was carried out combining processes at a NSR-2205i12D Nikon Stepper and a KSMA6 aligner (Süss MicroTech AG, Germany). Photoresists used were OIR 620-09 (0.6 μm) and HIPR-6512 (Fujifilm, USA), and LOR3A (Microchem Corp., USA). SU8 2005 was purchased from MicroResist Technology GmbH, Germany.

Optical microscopy images were obtained using a Leica DM4000 optical microscope. Scanning electron microscopy (SEM) and profilometry measurements were performed on an AURIGA (Carl Zeiss) and Dektak 150 (Veeco) respectively.

Electrochemical experiments were performed using a CH Instruments bipotentiostat (CH Instruments, Texas, USA) interfaced to a Windows XP-based PC. All experiments were conducted at $24 \pm 2^\circ \text{C}$.

Diffusion-controlled currents to interdigitated micro- and nanobands were simulated using Comsol Multiphysics 4.3 run on a Solaris workstation.

2.1. Design and fabrication

Cadence virtuoso layout editor (Cadence Design Systems, Bracknell, UK) was used to design 3 mm \times 3 mm chips featuring 2 sets of interdigitated microband structures. 5 different interdigitated structures were designed with the following band and gap widths: 400 nm, 500 nm, 1 μm , and 2 μm . The active area of the interdigitated structures is 500 $\mu\text{m} \times 500 \mu\text{m}$, and it is defined by a passivation layer which, in this case, consists of a 0.5–2 μm thick SU-8 photoresist layer. The microfabrication of these structures is similar to that of other microelectrodes reported in the past [21,48–50], but it differs in that a stepper performs the first lithographic step instead of the usual mask aligner. This change is important because while the use of a stepper allows the transfer of smaller patterns, it may complicate the correct alignment of subsequent photolithographic steps, involving the use of so-called “mix-and-match” processes.

Steppers allow for better resolution than photomask aligners due to their special optics. In conventional photomask aligners, the resist on a wafer is exposed once and all of the patterns featured in the photomask (usually a large number of chips) are transferred at once without size conversion. Steppers, on the other hand, use

Download English Version:

<https://daneshyari.com/en/article/742858>

Download Persian Version:

<https://daneshyari.com/article/742858>

[Daneshyari.com](https://daneshyari.com)